

University of Arkansas, Fayetteville

ScholarWorks@UARK

Chemical Engineering Undergraduate Honors
Theses

Chemical Engineering

5-2008

Exploring the potential for electromangetophoretic separation

Thomas Lewis

University of Arkansas, Fayetteville

Follow this and additional works at: <https://scholarworks.uark.edu/cheguht>

Citation

Lewis, T. (2008). Exploring the potential for electromangetophoretic separation. *Chemical Engineering Undergraduate Honors Theses* Retrieved from <https://scholarworks.uark.edu/cheguht/27>

This Thesis is brought to you for free and open access by the Chemical Engineering at ScholarWorks@UARK. It has been accepted for inclusion in Chemical Engineering Undergraduate Honors Theses by an authorized administrator of ScholarWorks@UARK. For more information, please contact scholar@uark.edu.

Exploring the Potential for Electromangetophoretic Separation

Author: Thomas W. S. Lewis

Advisor: Dr. Christa N. Hestekin

May 1, 2008

Current research in microfluidic technology is underway to develop automatic micro-analyzing chips for medical diagnostic testing. Diagnostic testing often requires separation of specific biological particles from a sample, and many of these molecules contain electric or magnetic properties. This project investigates the potential for separation in electromagnetophoretic and magnetophoretic microfluidic technology.

In electromagnetophoresis, the Lorentz force acting on a current carrying medium in a homogeneous magnetic field creates a pressure gradient in the fluid, resulting in an applied force to particles present in the separation medium. This force causes the particle to have a velocity component that is perpendicular to the medium flow and results in adsorption to the capillary wall. Since the force required for adsorption is size-dependent, particles can be separated based on size and electrical properties. In magnetophoresis, magnetic particles are separated by the application of an inhomogeneous magnetic field. Previous research by Watarai et. al. shows that polystyrene particles and red blood cells in a paramagnetic medium could be trapped in a silica capillary by the application of an inhomogeneous magnetic field to pressure-driven flow.⁹

Fused silica, a widespread material used in microfluidics, is an amorphous polymer made from silica dioxide (SiO_2) and silanol (SiOH) monomers. When exposed to a buffer solution, OH^- ions ionize SiOH to SiO^- , resulting in a negative capillary surface charge. The negatively charged capillary wall attracts cations present in the buffer solution, forming the electric double layer (EDL). When exposed to an external electric field, the cations in the EDL migrate towards the cathode, causing a bulk fluid motion. The resulting bulk flow can serve as a pump in microfluidic technology. In this project, EOF measurements were performed to explore its potential use in magnetophoretic technology.

INTRODUCTION

The concept of a micro-analyzing chip that could automatically perform diagnostic testing has led to the emergence of research in microfluidic technology. This so called lab on a chip (LOC) has the potential to drastically reduce the amount of resources necessary for diagnostic testing in medical applications. Since LOC's would not need expensive laboratories and highly trained technicians, it would revolutionize diagnostic testing accessibility in developing countries.¹ The development of disposable LOC's that do not require readers could also revolutionize at-home diagnostic testing and would significantly lower the cost of healthcare. This technology would also decrease the amount of time required to obtain diagnostic test results, enabling point of care testing.

Diagnostic testing often requires separation of specific biological particles from a sample and many of these molecules contain electric or magnetic properties. Differences in these properties between biomolecules provide a means by which they may be separated. Current technologies and research use electric fields (electrophoresis), magnetic fields (magnetophoresis), or the combination of both (electromagnetophoresis) to separate biological particles in solution. The technology of these separation methods could be combined with microfluidic chip technology to provide analytical separation at the microscale. This project will investigate the potential for separation in magnetophoretic and electromagnetophoretic technology.

Electrophoresis

Electrophoresis is the process by which charged particles are transported through a medium in an electric field. Differences in size and charge between molecules cause them to travel through the medium at different rates and subsequently cause separation. The rate at which separation occurs is directly proportional to the magnitude of the applied electric field, but large electric fields increase the amount of current. High current increases the amount of Joule heating, which has negative effects on the separation resolution due to natural convection and temperature effects on electrophoretic mobility.² A separation chamber of high surface area-to-volume ratio provides an efficient means of heat removal from the separation medium.² Capillary electrophoresis (CE) utilizes this effect and allows for the use of large electric fields in separation.

Electroosmotic flow (EOF) is another important factor in CE separation performance and is caused by the negative surface charge that exists on the capillary wall. Fused silica, the most widespread material used in CE capillaries, is an amorphous polymer made from silica dioxide (SiO_2) and silanol (SiOH) monomers.³ When exposed to a buffer solution, OH^- ions ionize SiOH to SiO^- , resulting in a negative capillary surface charge.³ The negatively charged capillary wall attracts cations present in the buffer solution, forming the electric double layer (EDL), which is displayed in Figure 1. When exposed to an external electric field, the cations in the EDL migrate towards the cathode, causing a bulk fluid motion. The affect of the bulk fluid movement on the observed electrophoretic mobility is represented as⁴

$$\mu_{obs} = \mu_{eff} + \mu_{eo} \quad (1)$$

where μ_{obs} is the observed electrophoretic mobility of the analyte, μ_{eff} is the effective mobility of the analyte, and μ_{eo} is the EOF mobility. The EOF mobility, which is dependent upon the zeta potential, is given by⁵

$$\mu_{eo} = \epsilon \zeta / \eta \quad (2)$$

where ϵ is the electric permittivity of the buffer, ζ is the zeta potential of the EDL, and η is the buffer viscosity. When an electric field is applied, the velocity that results is expressed as⁵

$$v_{eo} = \epsilon \zeta E / \eta \quad (3)$$

where E is the separation voltage per unit length.

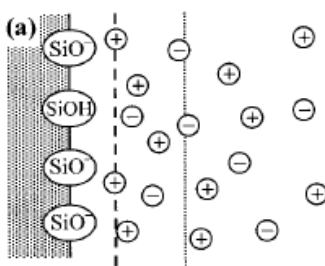


Figure 1. Diagram of ion interaction in EDL

In order to utilize EOF as an accurate separation technique in CE application, it must be measured and characterized with respect to the background electrolyte (BGE). The

distribution of cations near the capillary surface creates a potential profile in the radial direction which is described by the Poisson equation³

$$\nabla^2 \Psi = -\rho^* / \epsilon \quad (4)$$

where Ψ is the potential and ρ^* is the charge density. This expression can be expanded into the Poisson-Boltzmann equation, which is given by⁵

$$\frac{1}{(x+R)^n} \frac{d}{dx} \left((x+R)^n \frac{d\Psi}{dx} \right) = -\frac{e}{\epsilon} \sum_k z_k n_k^b \exp \left(-\frac{e z_k \Psi}{k_b T} \right) \quad (5)$$

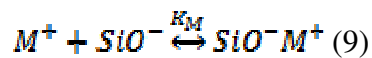
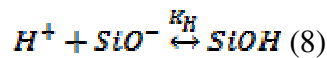
where n is the geometry parameter (n=0 for planar geometry and n=1 for axisymmetric geometry), e is the elementary charge, k_b is the Boltzmann constant, z_k are the ion valence numbers, T is temperature, and n_k^b are the bulk solution ion densities. The boundary conditions for this second order differential equation are $\Psi_{(x=d)} = \xi$ and $\frac{d\Psi}{dx}_{x=R} = 0$ ⁵. The Debye-Hückel approximation, which can be applied to dilute buffer concentrations, assumes that the zeta potential is less than 25 mV. This condition reduces the zeta potential from the Poisson-Boltzmann equation to³

$$\xi = \frac{\sigma \kappa^{-1}}{\epsilon} \quad (6)$$

where κ^{-1} is the Debye length (EDL thickness) and σ is the surface charge density of the capillary wall. If the expression for the zeta potential in Eq. #6 is substituted into Eq. 2, the following expression results³

$$\mu_{\epsilon\sigma} = \frac{\sigma \kappa^{-1}}{\eta} \quad (7)$$

Zhou and Foley utilized a site-dissociation – site-binding model to characterize the effects of buffer parameters on surface charge density and Debye length. In this model, the surface concentration of SiO^- is governed by the equilibrium that exists between the negatively charged silonate groups, hydrogen ions, and cations in solution. This equilibrium is dictated by buffer pH, cation valence number, ionic strength, ionic activity, and the dissociation constant. When hydrogen ions and monovalent cations come into contact with the silonate groups, they form immobile complexes of neutral charge and as a result reduce the surface charge density. These chemical interactions are represented as³



where $K_{H^+} = [SiOH]/a_{H^+}[SiO^-]$, $K_{M^+} = [SiO^-M^+]/a_{M^+}[SiO^-]$, and a is the activity of the individual species. Using these equilibrium constants, the surface charge density may be expressed as

$$\sigma = \frac{FQ_{0,a}}{1+K_M a_{M^+}+K_{H^+} a_{H^+}} \quad (10)$$

where F is Faraday's constant and $Q_{0,a}$ is the number of apparent silanol groups ($SiOH$, SiO^- , SiO^-M^+). A decrease in the number of hydrogen ions (increase in pH) results in a higher number of silonate groups. The resulting increase in surface charge density causes the EOF mobility to increase. Because silanol ions begin to dissolve into the buffer solution at pH values greater than 10, the charge density reaches a maximum value. Zhou tested this hypothesis by varying pH levels at a constant sodium ion concentration; these results are displayed in Figure 2a. Zhou also found that increasing the monovalent buffer concentration resulted in lower surface charge density, which can be seen in Figure 2b. Multivalent cations are capable of forming three-membered complexes and are more attracted to the capillary surface. Zhou found the EOF mobility of barium, a divalent ion, to be an order of magnitude lower than that of sodium; these results are displayed in Figure 3.

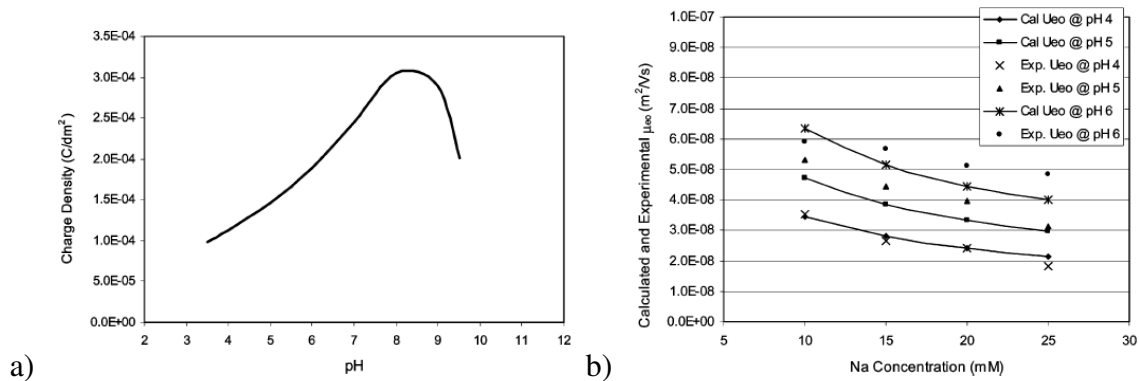


Figure 2. a) Monovalent buffer concentration effect on EOF mobility (Zhou and Foley)³
 b) pH dependence of surface charge density (Zhou and Foley)³

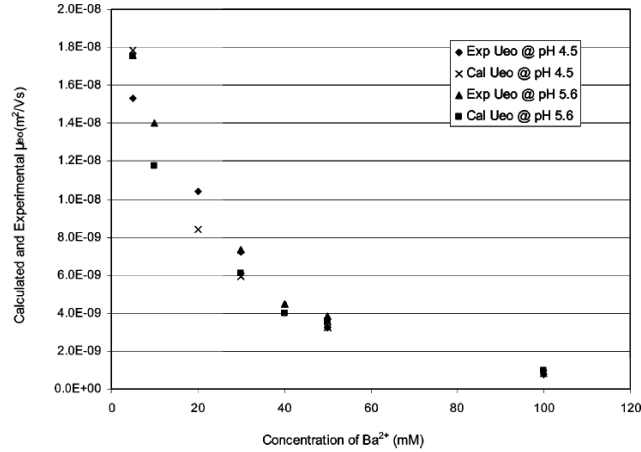


Figure 3. Divalent buffer concentration effect on EOF mobility (Zhou and Foley)³

In order to measure EOF mobility, Zhou used the five-step neutral marker method developed by Williams and Vigh.⁴ In the first step, a band of neutral marker is pressure injected and transferred by applying pressure. Next, a second neutral marker band is injected and transferred again by pressure. A voltage is then applied and the bands are allowed to migrate by EOF. In the last step, a third band is injected and moved by pressure to the UV detector. The retention time of the third band is used to calculate the pressure mobilization velocity by⁴

$$v_m = \frac{L_{eff}}{t_{N_3} + \frac{t_{inj}}{2} - t_d} \quad (11)$$

where L_{eff} is the effective length of the capillary, t_{N_3} is the retention time of the third peak, t_{inj} is the pressure injection time, and t_d is the delay time between steps. The pressure mobilization velocity along with retention time of the first two bands is used to calculate the distance traveled by the second band during the electrophoresis step. This value is calculated by⁴

$$L_{EO} = [(t_{N_2} - t_{N_1}) - (t_{N_2} - t_{N_1})]v_m \quad (12)$$

The resulting EOF mobility is then found using⁴

$$\mu_{EO} = \frac{L_{EO}L_t}{V_{prod}(t_{migr} - t_{ramp-up}/2 - t_{ramp-down}/2)} \quad (13)$$

Characterization and manipulation of electroosmotic flow can be used as a powerful tool in DNA CE separation, which is not size dependent in buffer solutions.⁶ In free-solution capillary electrophoresis (FSCE), separation occurs due to the balance of the electrical and drag forces acting on the analyte molecule. The electrophoretic mobility of an analyte molecule is the ratio of the particle velocity to the electric field strength, which may be represented as²

$$\mu = \frac{v_{ss}}{E} = \frac{q}{f} \quad (14)$$

where v_{ss} is the velocity of the analyte in the capillary, E is the applied electric field, q is the charge of the molecule, and f is the translational friction coefficient. For free-draining coil particles, such as DNA, the frictional coefficient is directly proportional to the number of base pairs.² Likewise, the charge of the DNA molecule is directly proportional to the number of base pairs.² Therefore, the electrophoretic mobility is not dependent upon the size of the DNA molecule and may be shown by²

$$\mu = \frac{q}{f} \sim \frac{N}{N} = N^0 \quad (15)$$

where N is the number of base pairs of the DNA molecule. End-labeled free solution electrophoresis (ELFSE) is the process by which a neutral molecule is attached to DNA, disrupting the constant charge to length ratio.⁷ McCormick et. al. showed that manipulation of the EOF could increase the size range of DNA that could be resolved using ELFSE separation in CE applications.⁷

Magnetophoresis

Magnetophoresis is a process by which magnetic particles are separated by the application of an inhomogeneous magnetic field. Hemoglobin present in red blood cells (RBC) contains iron, which causes the RBC to possess magnetic properties.⁸ When hemoglobin exists in a deoxygenated state, the bond between the heme group and the globin chain is ionic.⁸ The unpaired electrons in the deoxygenated hemoglobin cause the molecule to have a paramagnetic nature.⁸ In oxygenated hemoglobin however, the bonds are more covalent.⁸ Since there are not any unpaired electrons in the oxygenated hemoglobin, it is diamagnetic.⁸

The resultant force acting on magnetic particles in solution is the difference between the magnetic force acting on the particle and the electromagnetic buoyancy.⁹ This net force acting on the particle is represented by

$$F_m = F_p - F_f = \frac{V(\chi_p - \chi_f)}{\mu_0} \left(B \frac{dB}{dx} \right) \quad (16)$$

where V is the spherical particle volume, χ_p and χ_f are the magnetic susceptibilities per unit volume of the particle and the medium, μ_0 is the vacuum magnetic permeability and dB/dx is the magnetic flux gradient.⁹ The acceleration of the particle due to the magnetic force is counterbalanced against the drag force.⁹ This viscous force can be calculated using Stokes' Law, which is represented by

$$F_v = 6\pi\eta rv \quad (17)$$

where η is the viscosity of the medium and r is the particle radius.⁹

Watarai et. al. found that polystyrene particles and red blood cells in a paramagnetic medium could be trapped in the capillary by the application of an inhomogeneous magnetic field in the direction of the flow.⁹ The particles were able to be trapped when the magnetic force counterbalanced the viscous force.⁹ This was achieved through manipulation of countercurrent flow by a syringe pump.⁹ Balancing the forces from Eq. 16 and 17 allows for the calculation of the necessary flow needed for trapping and is represented by⁹

$$v = \frac{2(\chi_p - \chi_f)r^2}{9\mu_0\eta} \left(B \frac{dB}{dx} \right) \quad (18)$$

This project will observe the effects of EOF and medium choice on the trapping of polystyrene particles and red blood cells.

Pamme et. al. designed a microfluidic chip that could magnetophoretically separate particles of varying magnetic susceptibility and size.¹⁰ In this method, the separation was two-dimensional.¹⁰ Figure 4 displays the design of the lithographed glass chip that was used. An inhomogeneous magnetic field was applied in the y-direction and caused the inlet magnetic particles to be deflected.¹⁰ The amount of deflection depended upon the size and magnetic characteristics of the particles.¹⁰ The deflected particles then

exit the separation chamber through the outlet channels, causing separation of the particles.¹⁰

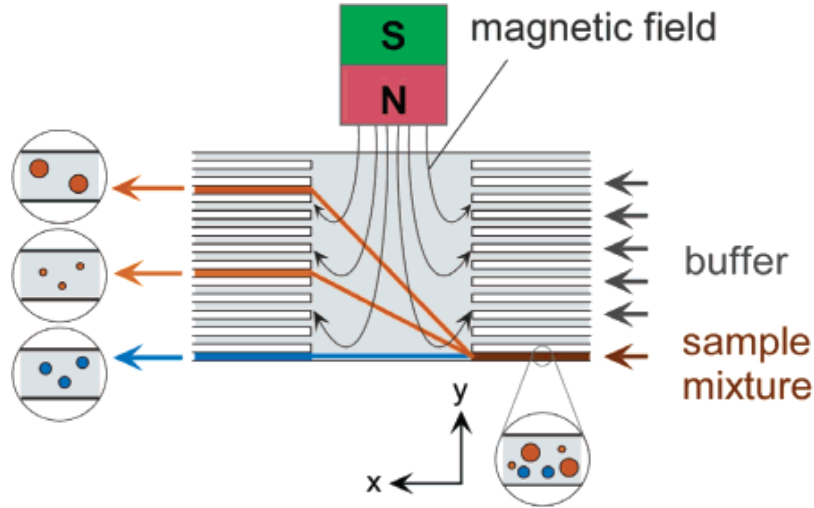


Figure 4. Diagram of the magnetophoretic separation chamber for the free-flow magnetophoretic chip¹⁰

Electromagnetophoresis

The application of a homogeneous magnetic field perpendicular to a current carrying medium causes the Lorentz force to act upon the medium and is the concept used in separation technique of electromagnetophoresis.¹¹ In electromagnetophoresis, the Lorentz force acting on the current carrying medium creates a pressure gradient in the fluid.¹¹ Watarai et. al. used this pressure gradient to manipulate the flow of polystyrene particles in the conductive medium. The net force acting on a particle in a medium is the sum of the electromagnetic buoyancy of the medium and the electromagnetic weight of the particle.¹¹ This force is given by

$$F_{EMP} = F_{EMW} + F_{EMB} = 2BV \left(\frac{\sigma_p - \sigma_f}{2\sigma_f - \sigma_p} \right) \frac{i}{S} \quad (19)$$

where B is the density of the magnetic flux, σ_p and σ_f are the electrical conductivities of the particle and the fluid, S is the inner area section of the particle, and i is the current.¹¹ This force causes the particle to have a velocity component that is perpendicular to the medium flow.¹¹ This electrophoretic velocity of the particle in a medium can be expressed as

$$v_{EMP} = \frac{4}{9} \left(\frac{\sigma_p - \sigma_f}{2\sigma_f + \sigma_p} \right) \frac{iBr^2}{S\eta C_w} \quad (20)$$

where C_w is the viscous drag coefficient due to the wall surface.¹¹ Watarai et. al. manipulated the electrophoretic velocity by changing the direction of the current periodically.¹¹ This in turn caused the electrophoretic velocity of the particle to vary and move in a zigzag manner.¹¹ This effect is displayed in Figure 5. The Lorentz force acting on the particles caused them to adsorb to the capillary wall.¹¹ The adsorption force was dependent upon the particle diameter and thus allows size-based separation to occur.¹¹ This project will observe the effects on the electromagnetophoretic separation of polystyrene particles in both buffer solution and polymer medium.

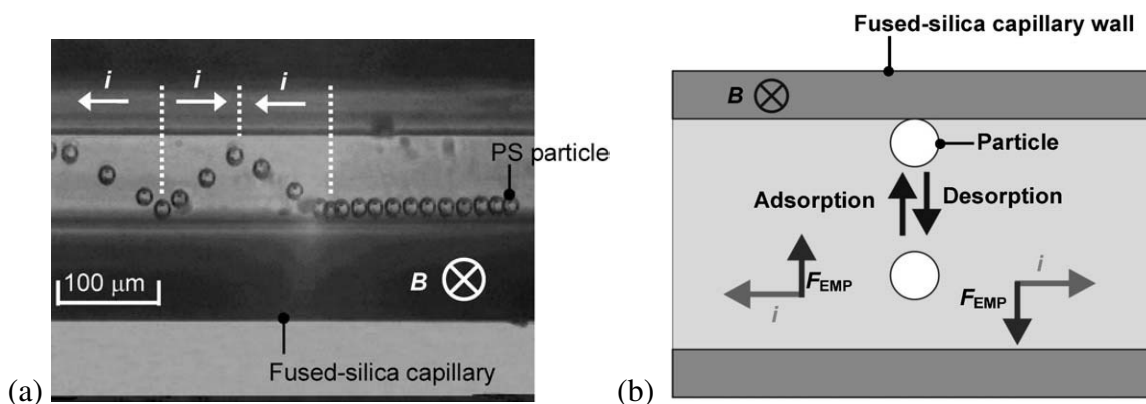


Figure 5.(a) Flow pattern of a typical polystyrene pattern in Watarai et. Al. experiment⁸
 (b) Diagram of forces acting on the polystyrene particles⁸

MATERIALS & METHODS

Potential Profile Modeling

The Poisson-Boltzmann equation (Eq. 5) was programmed into MATLAB to predict the effects of ion bulk density, ion valence number, and temperature on EDL potential profile. A zeta potential of 250 mV was used as the boundary condition for the EDL. The potential and the potential gradient were assumed to be zero at the capillary centerline.

EOF Measurement

A Beckman Coulter (Fullerton, California) P/ACE MDQ capillary electrophoresis system was used in the CE analysis of the EOF. Two methods were used in measuring the EOF: observation of polystyrene particle migration and the method developed by Williams and Vigh.⁴ For polystyrene particle analysis, fluorescent polystyrene particles with a size distribution of 2.5 – 4.5 μm diameter and nominal diameter of 4.1 μm were purchased from Spherotech (Lake Forest, Illinois). For these experiments, the laser signal was emitted at 488 nm and detection occurred at 520 nm. KCl, purchased from VWR (West Chester, Pennsylvania), was used to make 10 mM, 100 mM, and 1 M KCl solutions with respective pH values of 5.83, 5.89, and 6.17. Before injecting the sample, the capillary was washed with de-ionized water at 30 psi for 5 minutes. The capillary was then rinsed with the KCl buffer at 30 psi for 10 minutes. The sample was injected at 0.5 psi for 15 seconds. A 15 kV electric field was used to migrate the particles over a period of 200 minutes.

For EOF analysis using the Williams and Vigh method⁴, 5 μL benzyl alcohol, which was purchased from J. T. Baker (Phillipsburg, New Jersey), was added to 1.2 mL solutions of 10 mM KCl (pH = 5.83), 100 mM KCl (pH = 5.89), 1 M KCl (pH = 6.02), and 1 M KCl (pH = 9.63). A pressure of 2.0 psi for 5 seconds was used to inject the neutral marker bands. Transfer times of 1 minute at 2.0 psi were used during band separation. A 15 KV potential with 10 second ramp time was applied across the capillary over a 5 minute migration time. The samples were then analyzed using UV detection at 214 nm.

Magnetophoresis Apparatus Design

In order to create a non-homogenous magnetic field, $\frac{3}{4}$ " x $\frac{1}{2}$ " x $\frac{1}{8}$ " grade N42, nickel plated Neodymium block magnets were purchased from K&J Magnetics, Inc. (Jamison, Pennsylvania). The magnetic field was measured by gaussmeter model 907 purchased from Magnetic Instruments (Indianapolis, Indiana). The microfluidic chip used in the design contained a channel length of 85 mm and was purchased from Micralyne (Edmonton, Alberta, Canada).

RESULTS AND DISCUSSION

Potential Profile Modeling

The potential profiles for a 10 mM, 100 mM, and 1 M monovalent buffer solution are displayed in Figure 6. As the ionic density is increased, the thickness of the EDL decreases, resulting in a decrease in EOF. The higher buffer concentration increases the equilibrium number of $\text{Si}^- \text{M}^+$ complexes on the silica surface, which creates a steeper potential gradient profile. The effect of the ion valence number on the EDL thickness was observed for monovalent and divalent cations. These profiles are displayed in Figure 7 and show that increasing the ion valence number results in a decrease in EDL thickness. Since the divalent ions contain more charge, they feel a stronger attraction to the negatively charged surface, resulting in more $\text{Si}^- \text{M}^+$ complexes. Increasing the buffer temperature from 25°C to 100 °C resulted in a thicker EDL; this effect is shown in Figure 8.. The 100 °C calculation was used to exaggerate the effect of temperature in EDL, and could not be applied in CE work because it would increase the likelihood of bubble formation. The temperature increase causes increased Brownian motion, resulting in a thicker EDL.

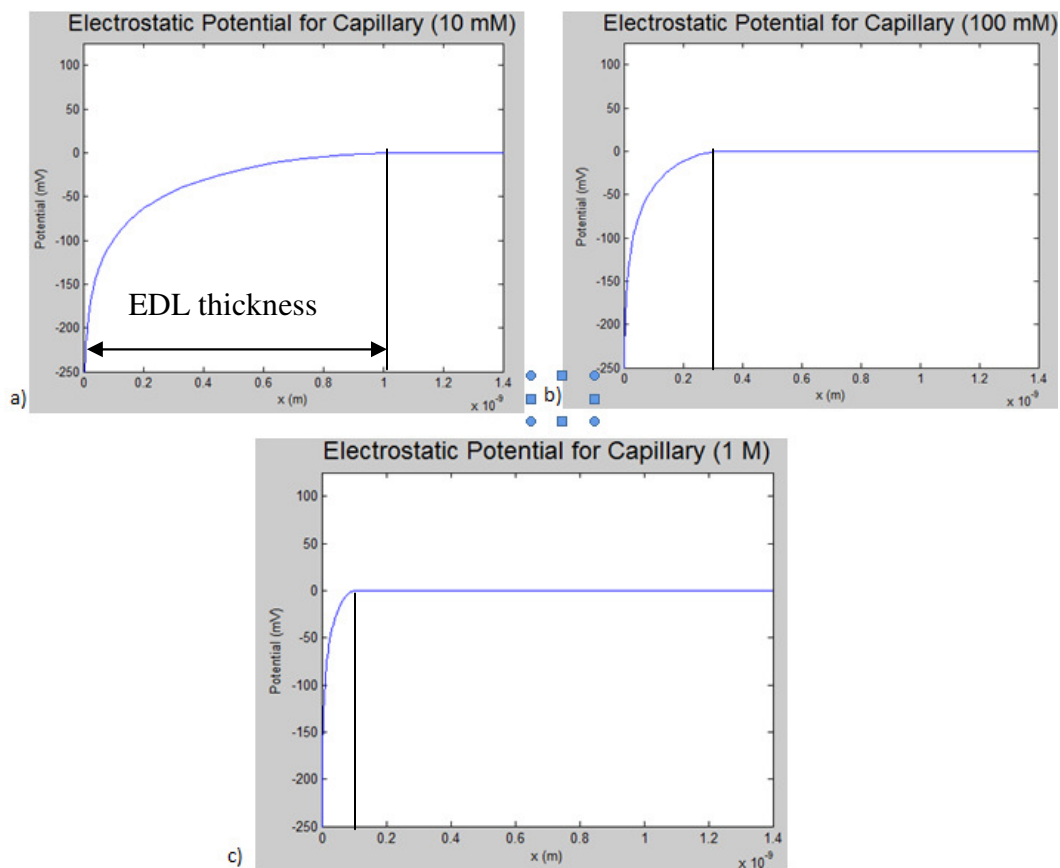


Figure 6. Bulk ion density effect on EDL potential profile for 10 mM (a), 100 mM (b), and 1 M (c) monovalent buffers

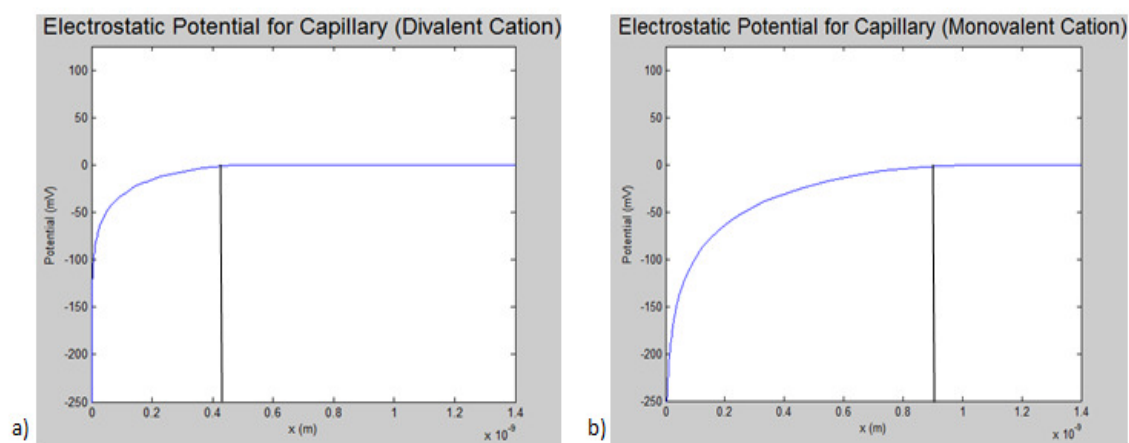


Figure 7. Ion valence number effect on EDL potential profile

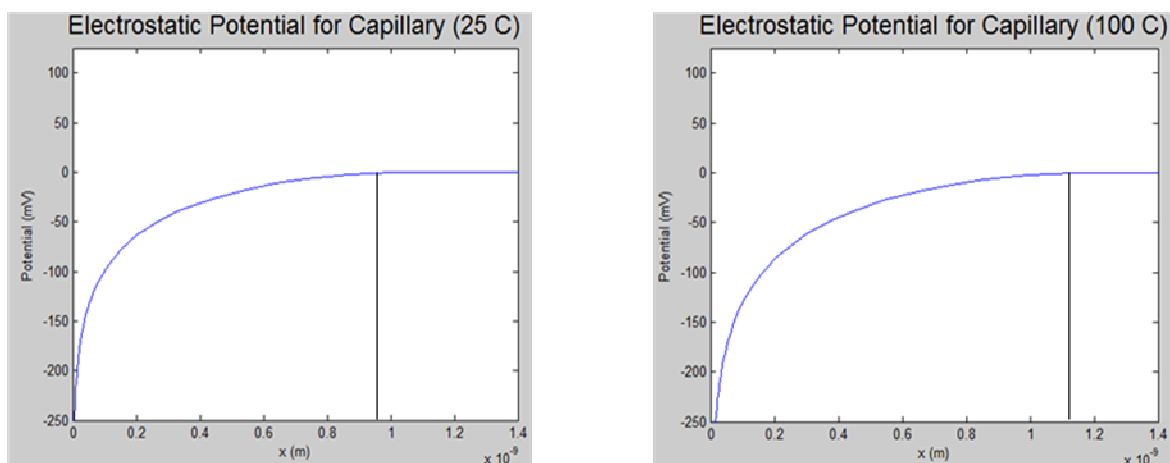


Figure 8. Temperature effect on EDL potential profile

EOF Detection

The timescale associated with the EOF particle migration was determined by performing capillary electrophoresis on the polystyrene particles. In order to determine the required time for particle migration by EOF, 200 minute runs were performed. The results from one of these runs are displayed in Figure 9. These results were then compared with runs performed using UV detection. One of the results from these runs is displayed in Figure 10. Runs using the fluorescent detector produced multiple narrow peaks, while the UV runs produced one broad peak. Multiple peaks in the fluorescent runs occurred because of the particle diameter distribution (2.5-4.5 μm). The results differ because of the manner of detection; fluorescent detectors only focus on a very narrow range of the capillary window, while UV detectors are see a much wider range.

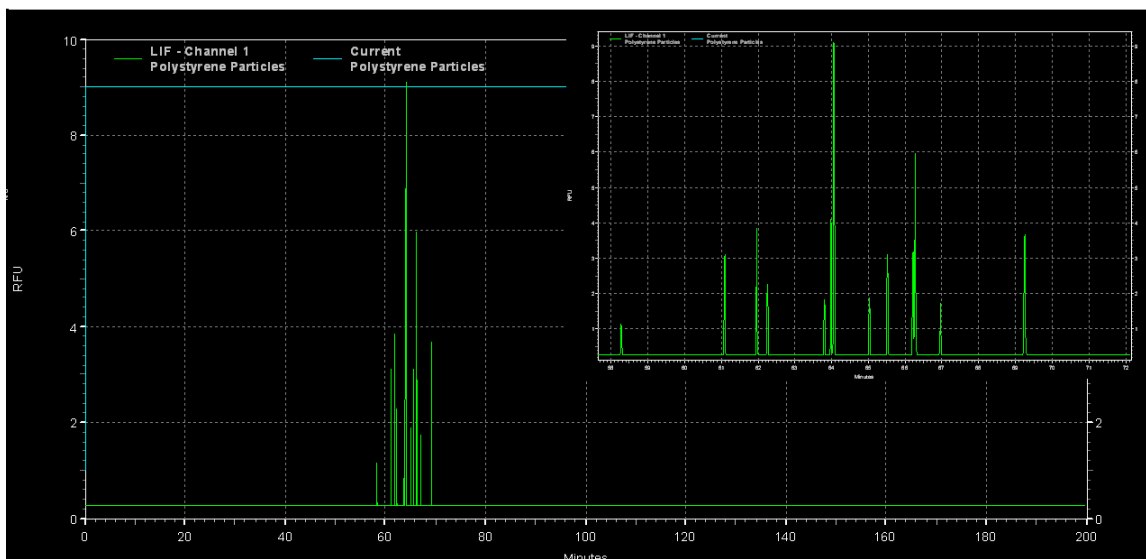


Figure 9. Observance of polystyrene migration using fluorescent detection

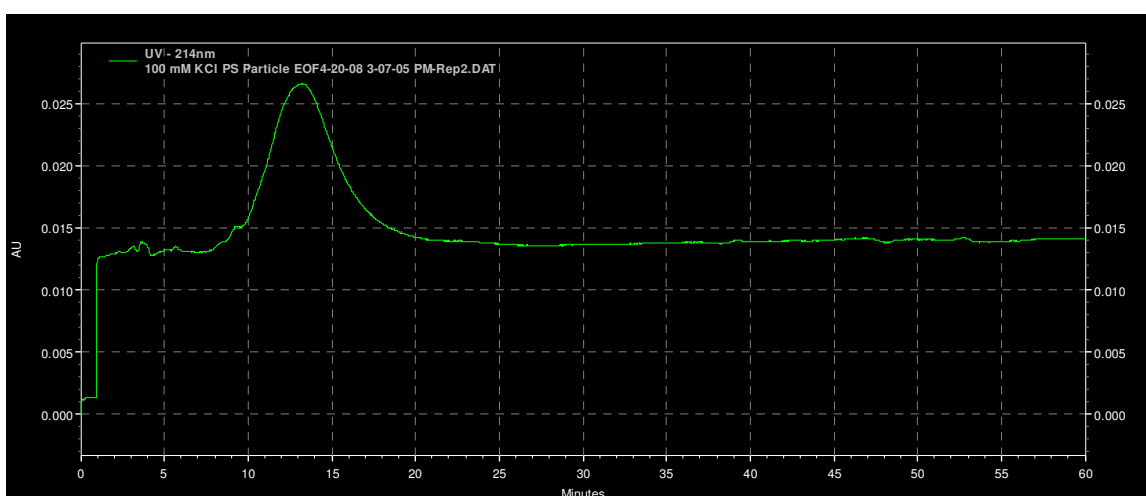


Figure 10. Observance of polystyrene migration using UV absorbance

In order to calculate the EOF for 10 mM, 100 mM, and 1 M KCl solutions, the method developed by Williams and Vigh was employed.⁴ Figure 11 displays an example of one the results obtained for a 10 mM run. The calculated electrophoretic mobilities are displayed in Table 1 and Figure 12. As buffer concentration was increased from 10 mM to 100 mM, there was an observed decrease in the EOF mobility, which is in accordance with results obtained by Zhou in Figure 2a. Further increase in buffer concentration to 1 M resulted in an increase in the electrophoretic mobility, which is inconsistent with Zhou's model. For the 1 M runs at 15kV, the current in the capillary exceeds that allowed

by the Beckman Coulter CE machine. Therefore, runs were performed at constant current, rather than constant voltage, making these results not comparable.

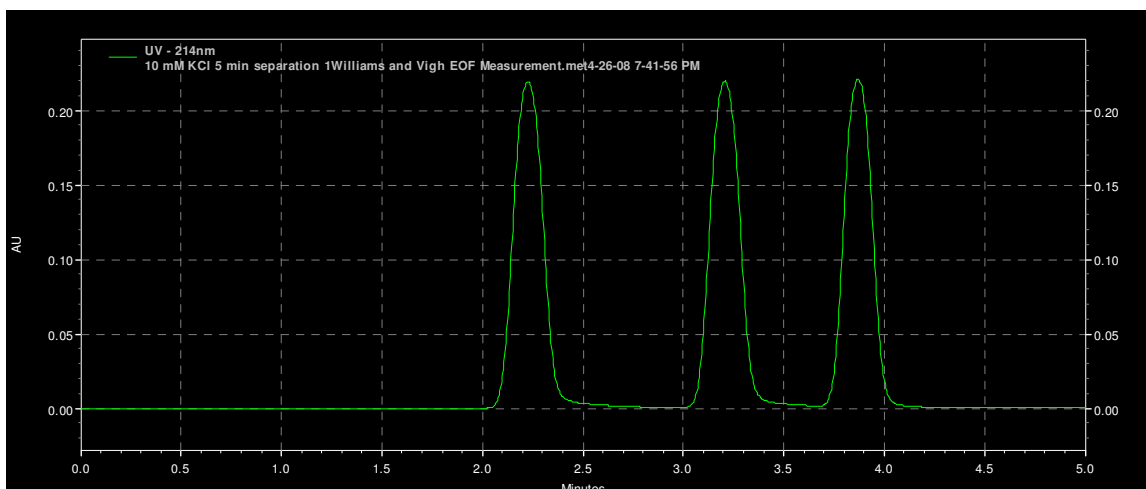


Figure 11. EOF mobility measurement using benzyl alcohol in 10 mM KCl

Table 1. Calculated EOF mobility and EOF velocity values for experimental runs

Benzyl Alcohol Neutral Marker	Run	Mobilization Velocity (m/s)	μ_{eo} (m^2/V sec)	v_{eo} (m/s)	Average Velocity (m/s)
10 mM KCl	1	2.56E-03	7.86E-09	8.25E-05	7.45333E-05
	2	2.55E-03	7.06E-09	7.41E-05	
	3	2.54E-03	6.38E-09	6.70E-05	
100 mM KCl	1	2.60E-03	7.02E-09	7.37E-05	7.37E-05
1 M KCl	1	2.56E-03	1.01E-08	1.06E-04	1.10E-04
	2	2.55E-03	9.76E-09	1.20E-04	
	3	2.52E-03	1.00E-09	1.05E-04	

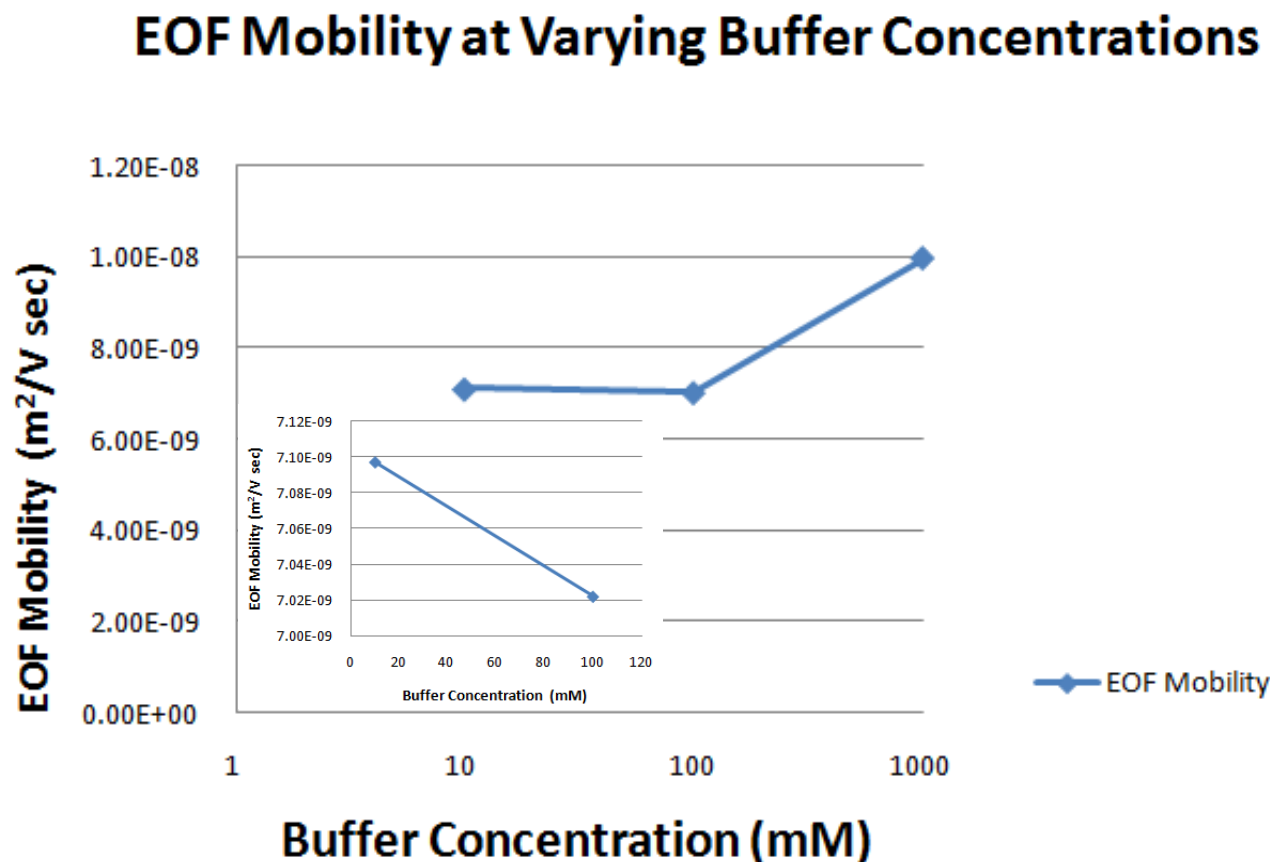


Figure 12. Effect of buffer concentration on EOF mobility

Magnetic Field Measurement

The magnetic fields produced by the Neodymium magnets were measured using the gaussmeter. The magnetic and $B \, \text{dB}/dx$ profiles for the 16 and 32 mm spacing are displayed in Figure 13. The magnetic profile is bell shaped as predicted by electromagnetic theory and is due to end effects of the rectangular magnets. The maximum $B \, \text{dB}/dx$ value for the 16 mm spacing was an order of magnitude larger than the 32 mm spacing. Since the magnetic spacing determines the maximum magnetic force that can act on a particle, the chosen spacing must create a large enough magnetic force

to balance the opposing viscous force. These values were used to design the magnetic spacing for the magnetophoretic apparatus, which is displayed in Figure 14.

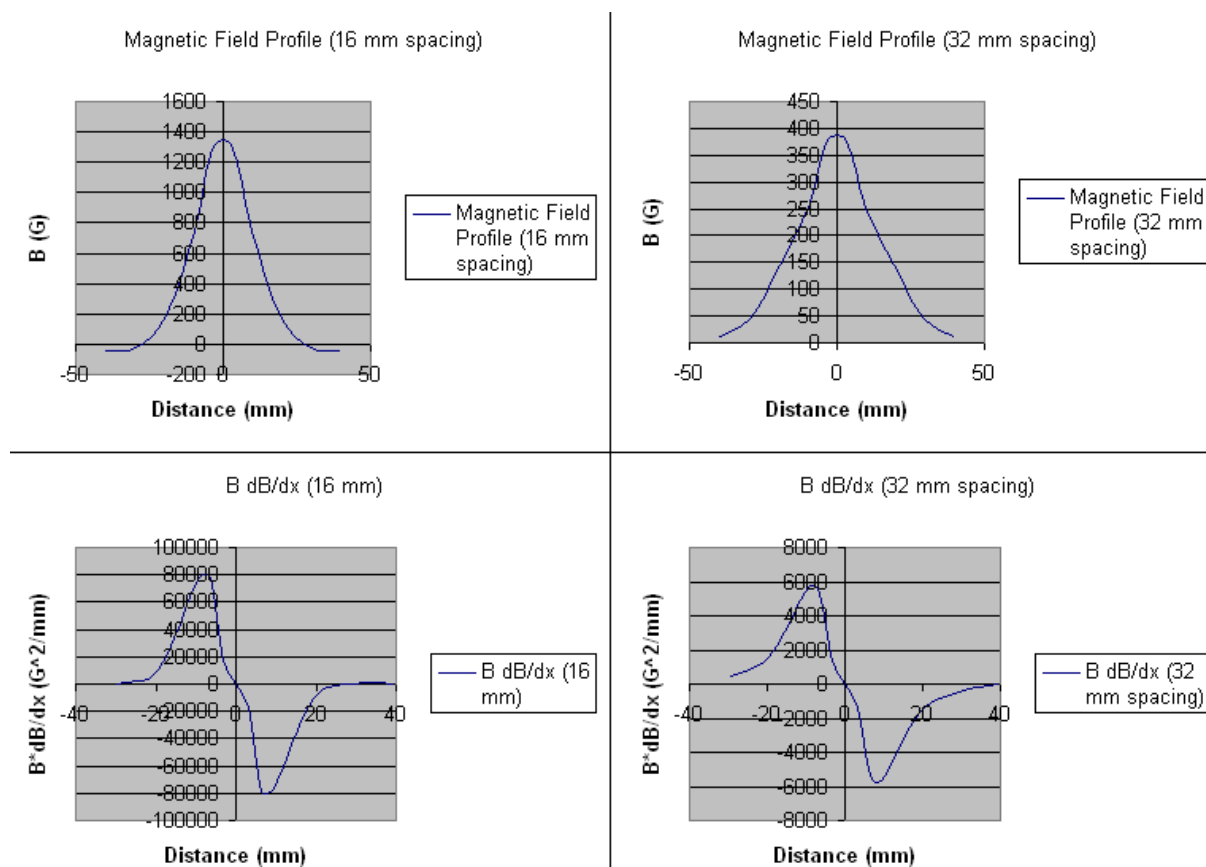


Figure 13. Magnetic measurements at 16 and 32 mm spacing

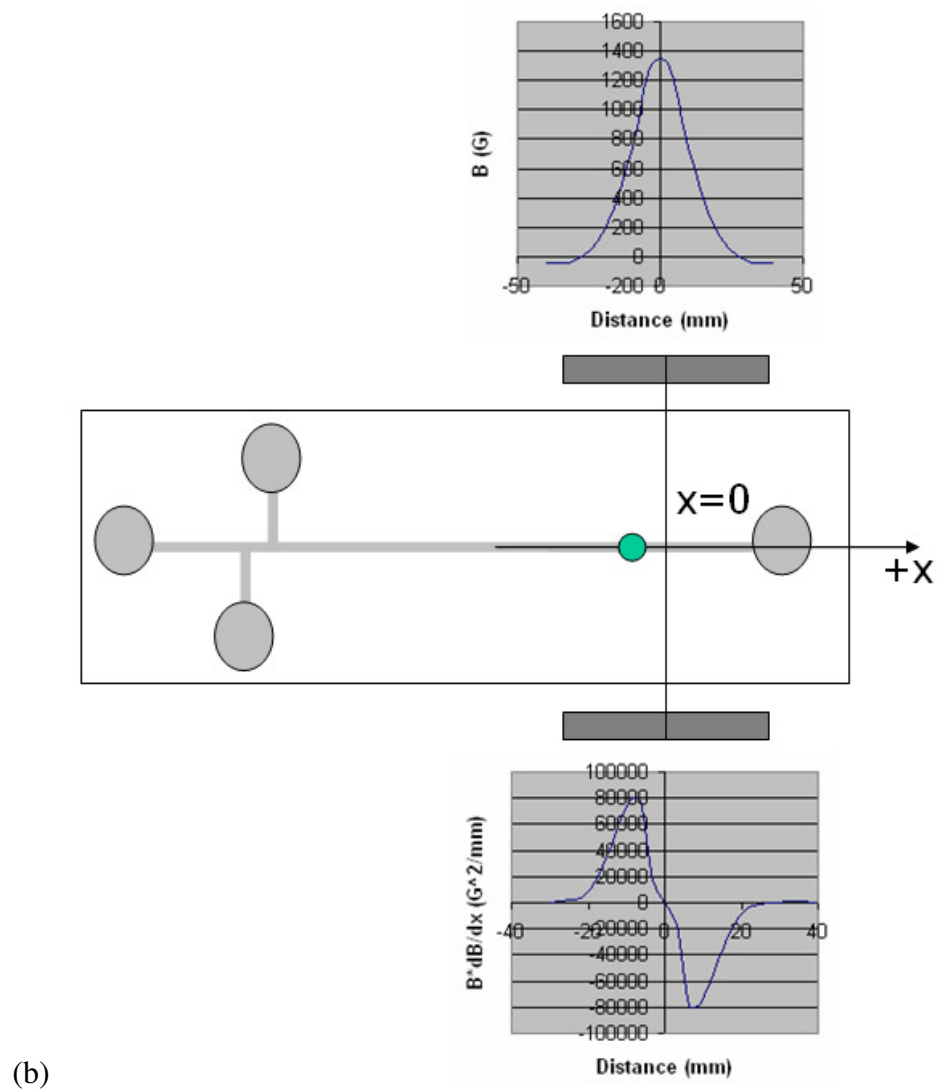


Figure 14. (a) Picture of designed magnetophoresis apparatus

(b) Diagram of magnetophoretic trapping

CONCLUSIONS AND FUTURE WORK

Experimental results for EOF measurement in 10 mM and 100 mM KCl runs were qualitatively in agreement with results obtained by Zhou. Since 1 M KCl runs were performed at constant voltage, the model employed by Zhou for predicting EOF behavior may not be applicable. Therefore, 1 M KCl EOF experiments should be performed at constant voltage. In order to determine the potential of applying EOF in magnetophoresis and electromagnetophoresis, EOF in a magnetic field should be measured and modeled. This modeling will have to consider the effects of the Lorentz force acting on the charged particles. Also, the effect of varying the current profile in electromagnetophoresis should be observed experimentally. If the current profile is imbalanced, there could be a resulting net EOF flow. Therefore, the use of a syringe pump, which increase leakage in microfluidic chips, would not be required. An example of a current profile that could be utilized is displayed in Figure 15.

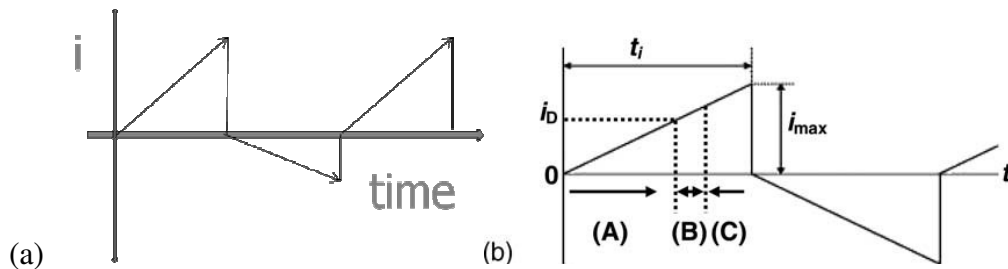


Figure 15. (a) Current profile that could be applied in future research
 (b) Current profile applied to electromagnetophoresis device by Watarai et. al.¹¹

References:

1. Yager, P., Edwards, T., Fu, E., Helton, K., Nelson, K., Tam, M. R., Weigl, B. H., *Microfluidic diagnostic technologies for global public health*. Nature, 442 (27), July 2006, p. 412-418.
2. Grossman, P. D., Colburn, J. C., *Capillary Electrophoresis Theory and Practice*, Academic Press Inc., 1992, San Diego, California.
3. Zhou, M. X., Foley, J. P., *Quantitative Theory of Electroosmotic Flow in Fused-Silica Capillaries Using an Extended Site-Dissociation – Site Binding Model*. Anal. Chem. 2006, 78, 1849 – 1858
4. Williams, B. A., Vigh, G., *Fast, Accurate Mobility Determination Method for Capillary Electrophoresis*, Anal. Chem., 1996, 68, 1174 – 1180
5. Berli, C. L. A., Piaggio, M. V., Deiber, J. A., *Modeling the zeta potential of silica capillaries in relation to the background electrolyte composition*, Electrophoresis 2003, 24, 1587 - 1595
6. Razee, S., Tamura, A., Masujima, T., *The effect of a crossed magnetic field on capillary electrophoresis*. Chem. Pharm. Bull., 42 (11), p. 2376-2378.
7. McCormick, L. C., Slater, G. W., *A theoretical study of the possible use of electroosmotic flow to extend the read length of DNA sequencing by end-labeled free solution electrophoresis*. Electrophoresis 2006, 27, p. 1693-1701.
8. Zborowski, M., Osera, G.R., Moore, L. R., Milliron, S., Chalmers, J. J., Schechter, A. N., *Red Blood Cell Magnetophoresis*. Biophysical Journal, 84, April 2003, p. 2638-2645.
9. Watarai, H., Namba, M., *Capillary magnetophoresis of human blood cells and their magnetophoretic trapping in a flow system*. Journal of Chromatography A, 961 (2002), p. 3-8
10. Pamme, N., Manz, A., *On-chip free-flow Magnetophoresis: Continuous Flow Separation of Magnetic Particles and Agglomerates*. Anal. Chem. 2004, 76, p. 7250-7256.

11. Watarai, H., Suwa, M., Iiguni, Y., *Magnetophoresis and electromagnetophoresis of microparticles in liquids*. *Anal. Bioanal Chem* (2004), 378, p. 1693-1699.
12. Wang, W., Zhou, F., Zhao, L., Zhang, J. R., Zhu, J. J., *Measurement of electroosmotic flow in capillary and microchip electrophoresis*. *J. Chrom. A*, 2007, 1170 (1-2), 1-8